Andrzej Wilk, Władysław Koc, Cezary Specht, Jacek Skibicki, Slawomir Judek, Krzysztof Karwowski, Piotr Chrostowski, Jacek Szmagliński, Paweł Dąbrowski, Krzysztof Czaplewski, Mariusz Specht, Roksana Licow, Sławomir Grulkowski

Innovative mobile method to determine railway track axis position in global coordinate system using position measurements performed with GNSS and fixed base of the measuring vehicle

Abstract

The shape of the railway track axis and its position in the global coordinate system are essential when defining design parameters of the railway. Correct reconstruction of these quantities is vital for both verifying the compliance of real track parameters with the design and for diagnosing, as all track deformations can also be defined as deviations of real parameters from their design values. The measurements of quantities related to the railway track geometry can be divided into global and local ones. Global measurements determine the position of elements in the global system of geographic coordinates, while local measurements give relative positions of elements with respect to other elements (e.g. lateral inclination at a given kilometre of the railway track) or temporary deviation of parameters from their assumed value (e.g. various track deformations). Depending on the applied measuring method, either global or local parameters are determined, or both of them simultaneously. The article proposes an innovative method to determine the railway track axis position, which makes use of Global Navigation Satellite Systems (GNSS) receivers distributed in such a way as to form a geometric constraint called the fixed base. The analysis of theoretical properties and metrological attributes of the fixed base is presented. All theoretical analyses have been verified experimentally.

Key words: position measurements performed with GNSS, inclinometry, railway track axis, geometric layout of the track

1. Introduction

The shape of the railway track axis and its position in the World Geodetic System (WGS) reference frame are essential parameters defining the railway line. Precision in determining railway track coordinates and other characteristic parameters are crucial for its durability and reliability, as well as for possible speed limits to be reached by trains running on it. The main problems faced during the operation of railway lines are related to traffic safety in the context of rapid failure (e.g. derailment), to the noise and vibrations generated by the moving train, as well as to accelerated wear of rolling stock and infrastructure [1-5]. Hence, continuous progress is observed in methods for determining the track axis, both for construction and diagnostic purposes. The measurements of quantities related to the railway track geometry can be divided into global and local ones. Global measurements determine the position of elements in the global system of geographic coordinates, while local measurements give relative positions of elements with respect to other elements (e.g. lateral inclination at a given kilometre of the railway track) or temporary deviation of parameters from their assumed value (e.g. various track deformations) [5–9].
Currently used methods of determining the track axis can be divided into three groups:
  a) The first group includes manual measurements performed with the use of traditional geodetic methods and optionally using satellite techniques. This group also includes all kinds of manually driven measuring trolleys, equipped with relevant measuring instruments. These methods allow us to obtain measurement results which are local in nature, i.e. in the coordinate system related to the rail track, and, in the case of using satellite techniques, also global results, i.e. in one of the coordinate systems of the global positioning system. The common feature of these methods is high measurement precision (both with regard to results

of local and global nature) with limited efficiency, i.e. slow pace of the measurement (typically from 0.1 to approx. 1 km/h), which translates into significant costs. For example, in [10] a GNSS receiver attached to a manually operated trolley was used, achieving in determining the position of the track axis, the accuracy at the level of several millimetres. A similar solution with a hand-operated trolley was used in [11], except that three GNSS receivers mounted in a known spatial configuration were used. The accuracy of determining the position of the track axis was obtained at the level of 2 mm. This was possible thanks to the use of three receivers, but also due to the dense network of Real Time Kinematic (RTK) reference stations located along the railway line which was examined. Other teams carrying out measurements with the use of manual trolleys achieve similar results [12, 13].

b) The second group of railway track measurement methods comprises automatic measurement systems installed on diagnostic vehicles and making use of satellite technique in combination with other instruments checking the track surface condition. The measurements belonging to this group are characterised by high accuracy in determining local and lower global parameters, and slightly higher efficiency, compared to manual methods. Typically, measurements are performed at the pace of 3 to 5 km/h, using hand-pushed or self-propelled trolleys, or using a combination of base and satellite vehicles. The last solution was used in the construction of the EM-120 SAT measuring draisine [14, 15]. The use of a two-vehicle system made it possible to measure local deviations of track parameters with the accuracy of 1 mm, but it is possible to locate them in the global system with the accuracy of 40 cm.

c) The third group includes all types of measuring trains and draisines used for diagnostic checks of railway track surface condition. As a rule, these vehicles move at relatively high speeds, from about 50–60 km/h to as much as 250 km/h and more. Consequently, the measuring efficiency of the methods comprising this group is very high, but high accuracy of measurement is only achieved for local parameters. Global parameters, if recorded, are only used for spatial positioning of local measurements. The LIMEZ III diagnostic vehicle used by German railways [16], the "Doctor Yellow" diagnostic train of Japanese railways [17–19] and a number of vehicles used by other railway authorities [20–24] constitute examples of applied solutions.

An important change in railway track measurements took place thanks to methods making use of satellite navigation and reference stations. Their grid currently covers the area sufficient for calculating corrections in many countries worldwide. Operating in real-time (RTK and Real Time Network – RTN) mode, the position measurement methods using GNSS with coordinate correction make it possible to perform very efficient and highly accurate measurements of railway track coordinates [25–29]. This system is the basis for the new method of determining the rail track axis, which is proposed in this paper. Due to its innovative character, the proposed method cannot be included in any of the earlier described groups of measuring methods. It makes it possible to determine both global and local parameters with very high accuracy (the measurement precision slightly worse than the methods of the first group), at a relatively high target measuring pace, of 30–40 km/h, i.e. only slightly lower than that characteristic for methods belonging to the third group. In the second chapter the theoretical base of the method was described, and in the third chapter the results of verification experiment are presented. The fourth chapter contains conclusions.

2. Assumptions of the proposed measuring method

The proposed measuring method is based on mobile position measurements performed with GNSS and makes use of a typical 4-axis freight wagon-platform equipped with two GNSS receivers installed above the pivot pins of the two bogies. For a bogie wagon, it is reasonable to assume that the bogie pivot axis always points at the track axis. Therefore, installing the receivers in the above-mentioned way ensures that they will record the real position of the railway track axis during the wagon motion.

2.1. Concept of fixed base

Although, theoretically, one GNSS receiver is enough to determine the track axis coordinates, the use of two receivers mounted at a fixed distance from each other offers a number of advantages, with respect to functionality of the system and it's metrological properties. The distance between the fixing points of these two receivers defines the so-called fixed base of the measuring system. Its length A is equal to the distance between bogie pivot axes, as shown in Fig. 1.
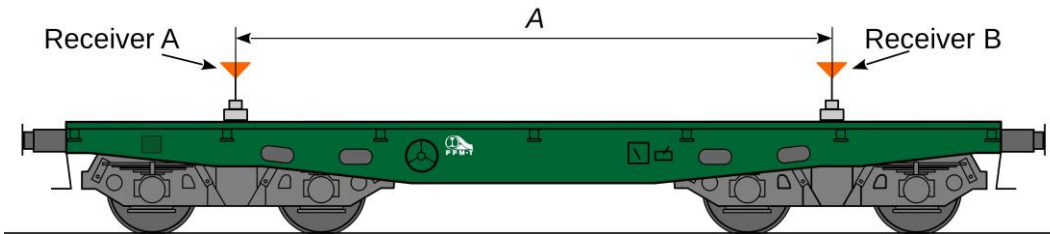

Fig. 1. Fixed base of the measuring wagon

The length of fixed base is strictly dependent on the wagon construction. With regard to further considerations, the greater length of fixed base translates into greater precision in determining the wagon spatial orientation, therefore, the longest possible wagon should be used. In turn, the required accuracy of the receivers positioning, i.e. the precision of determining the length of the fixed base, should be within lower order of magnitude than the uncertainty of determining the position with the use of GNSS receivers.

2.2. Range of supplementary measurements

According to the definition, the track axis should be determined at the rail head level. Consequently, the GNSS receivers recording satellite signals should be installed in such a way that the phase centres of their antennas are situated at this level. Technically, this arrangement is not possible, and the receivers are installed at the height of about 1.5 m above the rail head level. As a result all the coordinates recorded by the receivers have to be corrected. When the measuring platform moves along a straight and horizontal track section, this correction is not needed, but when it approaches hills or, what is more important, moves along a horizontal arc, where lateral track inclinations always occur, the coordinate values recorded by the receivers differ from those defining the current wagon position. Calculating corrections requires the information on current lateral and longitudinal tilts of the measuring wagon with respect to the direction of motion. Moreover, it should be kept in mind that the accuracy of determining the railway track axis is also affected by clearances between wheel rims and rolling surface of the rail, and constructional clearances characteristic for a given type of wagon. Because of these clearances, the bogie pivot axis can move laterally with respect to the direction of motion and does not always coincide precisely with the railway track axis. Possible pivot axis displacements can be reach as much as several centimetres. Therefore to obtain high-accuracy results, supplementary measurements of wagon bodywork position with respect to the rolling rail surface should be performed. These measurements will allow for calculating relevant corrections.

2.3. Metrological functionality of fixed base

The fixed base simplifies a number of procedures indispensable for obtaining correct results of railway track axis measurement in the global coordinate system. It is also used to assess the inaccuracy of position determination in dynamic conditions, as it makes it possible to orientate the wagon position in the global reference system before calculating the required coordinate correction values. Finally, it can also be used for assessing moving stability of the measuring wagon.

2.3.1. Assessing the uncertainty of coordinate measurement

Each GNSS receiver gives its position in the form of latitude and longitude values. However, the latitude/longitude coordinate system is not the Cartesian system, but it maps the spherical shape of the Earth. Therefore, for the GNSS measurements to be applicable in practical implementations, the latitude and longitude values should first be converted into the so-called global Cartesian coordinate system YX, which is represented in Poland by the Gauss-Krueger projection for the ellipsoid GRS 80, with axial longitudes 15ºE, 18ºE, 21ºE and 24ºE.

Hence, each receiver defines its position by two coordinates: The *Y*-coordinate responsible for orientation in the East-West axis direction, and the *X*-coordinate for the North-South axis direction. When the measuring wagon is in motion, all the measurements are, by their nature, single measurements. Assessing the uncertainty level of these measurements is very difficult, as this uncertainty will depend on current configuration of satellites and on the GNSS receivers' ability to observe them, as a result of which it will never be constant. However, the fixed base of known length *A* can be used for assessing the uncertainty level of position measurement, by comparing the fixed base length obtained from an independent measurement with that calculated from position measurements performed with the use of GNSS. This comparison should be made in statistical terms using the modified method to determine standard deviation according to the procedure presented below.

Since the GNSS receivers work synchronically, for each measurement two pairs of coordinates (Y_A, X_A) and (Y_B, X_B) are recorded. Therefore, for each measuring step, the fixed base length can be calculated, according to the relation:

$$A_{ps} = \sqrt{(X_A - X_B)^2 + (Y_A - Y_B)^2} \quad (1)$$

The value of A_{ps} given by formula (1) should be identical to the fixed base length *A* determined in an independent manner. However, this comparison can only be made for the situation when the measuring wagon moves on the horizontal track. When moving up or downhill, apparent shortening of the base length calculated from position measurements performed with GNSS will be observed, it is due to perspective foreshortening, as shown in Fig. 2.
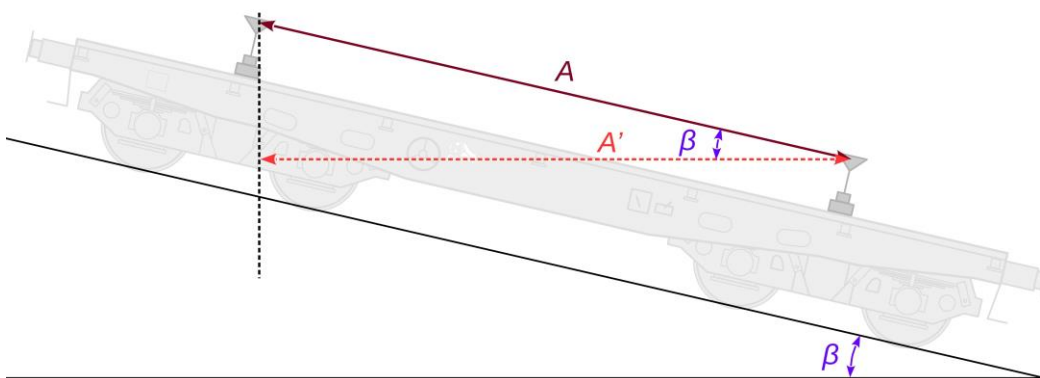

Fig. 2. Apparent shortening of fixed base length when the measuring wagon moves up or downhill

Figure 2 shows that when the measuring wagon moves up or downhill at the inclination angle β, the fixed base length *A*, reduced to the horizontal level, is shortened to the length *A'* given by the formula:

$$A' = A \cdot \cos \beta \quad (2)$$

For these cases, the value A_{ps} obtained from formula (1) should be compared with the value A' given by formula (2).

Since the dynamics of longitudinal track inclination changes is very small in railway conditions, it can be assumed, for limited speeds of the measuring wagon motion, that collecting minimum data needed for statistical analysis takes place during the time in which the inclination does not change considerably (for speed $v = 30$ km/h and receivers' sampling frequency $f = 20$ Hz, the minimum number of $n = 30$ measurements are collected in 1.5 s, during which time the measuring wagon covers the distance of 12.5 m). In those conditions, the standard uncertainty of a single measurement can be assessed from the estimate of standard deviation of the fixed base measurement obtained from position measurements by GNSS A_{ps} (formula (1)) with respect to the mean value of this length obtained from independent measurements according to formula (2). The best form of the standard deviation estimate is the experimental standard deviation, which, for the adopted assumptions, is given by:

$$s_{A_{ps}} = \sqrt{\frac{1}{n-1} \cdot \sum_{i=1}^{n} \left(A_{ps\,i} - \overline{A'}\right)^2} \quad (3)$$

where: n – number of measurements in terms of statistics; $A_{ps\,i}$ – i-th measurement of fixed base length calculated from satellite data; A' – mean of fixed base length measurements obtained from independent measurements.

The experimental standard deviation given by formula (3) allows not only for taking into account the stochastic spread of satellite positioning results, but also for detecting systematic errors, which may appear as a result of long-lasting asymmetric visibility of satellites (for instance, they can be seen only in one section of the sky). This would be impossible for the experimental standard deviation calculated with respect to the mean A_{ps} from satellite measurements.

Certainly, the final uncertainty of satellite position measurement should also include the uncertainty of determining of fixed base length A and angle β, which results from the uncertainty of calibration of the used measuring devices. The final value of standard uncertainty of satellite coordinate determination, before converting the coordinates in the rail head level, is given by the formula:

$$u(X_A) = u(Y_A) = u(X_B) = u(Y_B) = \sqrt{(s_{A_{ps}})^2 + u(A')^2} =$$

$$= \sqrt{\frac{1}{n-1} \cdot \sum_{i=1}^{n} \left(A_{ps\,i} - \overline{A'}\right)^2 + \cos^2 \beta \cdot u(A)^2 + (-A \cdot \sin \beta)^2 \cdot u(\beta)^2} \quad (4)$$

2.3.2. Compensating the effect of dynamic movements of the measuring wagon on measurement results

Dynamic movements of the measuring wagon include low-frequency movements, such as lateral and longitudinal tilts resulting from the presence of hills and lateral inclinations of the track, and high-frequency movements, generated by geometric imperfections of the track. Direct use of the fixed base is not necessary to compensate the effect of these movements on the measurement results. However, its use facilitates re-calculation of the obtained corrections into the global reference system.

Compensating longitudinal tilt

When the measuring wagon moves up or downhill, its position determined by GNSS receivers differs by some length from the real position of the measuring wagon, as shown in Fig. 3.
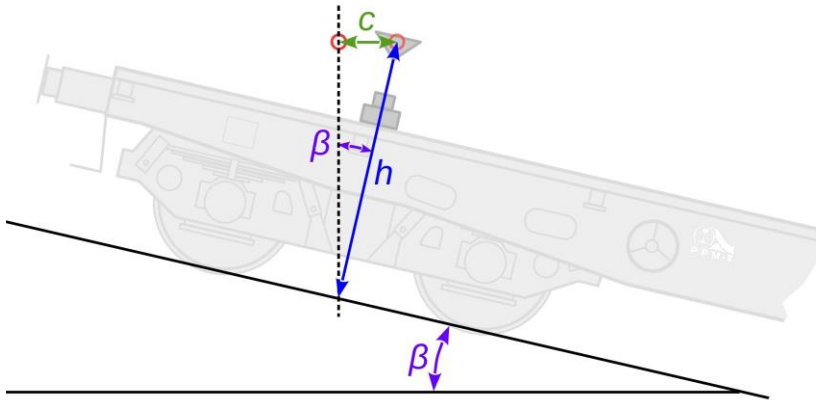
Fig. 3. Compensating longitudinal tilt of the measuring wagon

The value of the longitudinal tilt correction c can be calculated based on the measured longitudinal inclination angle β of the track, and the known height h of the receiver's position above the rail head plane, according to the formula:

$$c = h \cdot \sin \beta \quad (5)$$

Assuming that the receiver is placed at the height $h = 1.5$ m, the value of correction c for the steepest track inclinations which may exist on railway lines (i.e. 50–70‰) does not exceed 10 cm. In the majority of cases, this value will be less than 5 cm. Although small in magnitude, the correction c should be taken into account if high precision of measurements is expected, especially in the simultaneous presence of lateral tilt of the wagon.

Compensating lateral tilt

Compensation of lateral tilt, which includes corrections resulting from track inclination on arcs and from wagon motion fluctuations caused by track unevenness, is a similar issue to the compensation of longitudinal tilt, but slightly more complex. This difference results from various definitions of real and design track axes. The design track axis is the circular projection of the real axis on the horizontal plane, with the rotation axis situated on the lower edge of the railway sleeper, on the inner side of the arc. The principle of compensation is shown in Fig. 4.
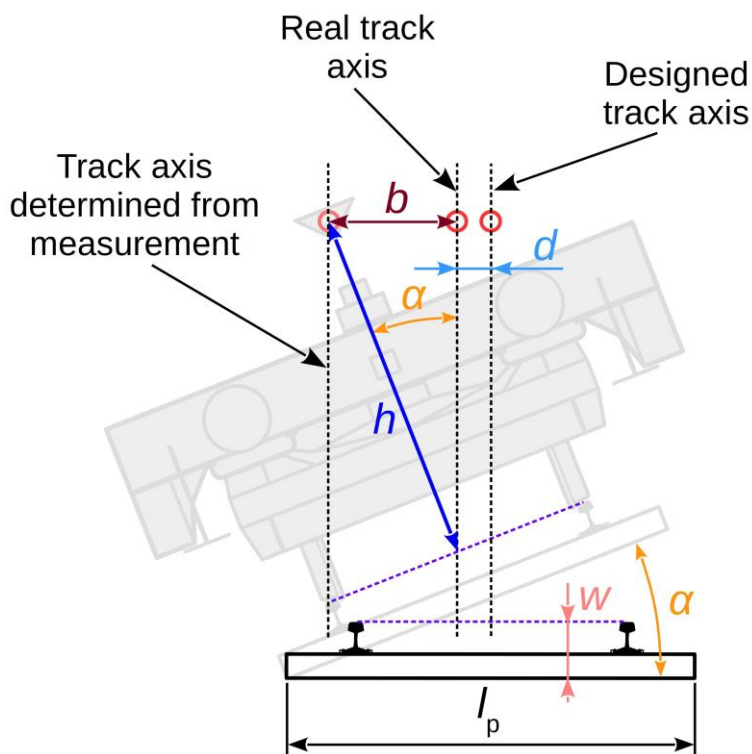
Fig. 4. Compensating lateral tilt of the measuring wagon (description in the text)

The tilt of the measuring wagon on the arc, caused by lateral track inclination of the angle α, makes results in the track axis obtained from the measurement being shifted inwards at the length b with respect to the real axis position. To determine the design axis position, we should also take into account the nonsymmetric track rotation, the centre of which is situated, for technological reasons, on the lower edge of the railway sleeper. The difference between the positions of real and design axes is marked as the distance d in Fig. 4. The distance b can be calculated from the formula similar to formula (5):

$$b = h \cdot \sin \alpha \quad (6)$$

The distance d is directly related to the railway track structure, as it is calculated from the known length l_p of the railway sleeper, the design height w of the track structure (rail, sleeper, and rail fixing to the sleeper), and the angle α resulting from the wagon tilt. The formula linking these quantities is as follows:

$$d = \begin{cases} \dfrac{l_p}{2} \cdot (1 - \cos \alpha) + w \cdot \sin \alpha & \text{for} \quad \alpha \geq 0 \\[2ex] -\left[\dfrac{l_p}{2} \cdot (1 - \cos \alpha) + w \cdot \sin |\alpha| \right] & \text{for} \quad \alpha < 0 \end{cases} \quad (7)$$

Depending which track axis (real or design one) is to be obtained from the measurement, only correction b or the sum of corrections $b + d$ is applied.

Compensation of lateral wagon displacements

Lateral displacements of the measuring wagon are the result of the presence of clearances between wheel rims and the rail head surface, and of the possible changes of track width, which is increased, for instance, on small-radius arcs. In extreme cases, lateral displacements can reach as much as 2–3

cm. Therefore, to ensure high precision of measurements, these displacements should be measured and a relevant correction introduced. To calculate this correction, permanent monitoring of the distance between the two track rails is required, along with the measurement of wagon body position with respect to one of the rails, as shown in Fig. 5.
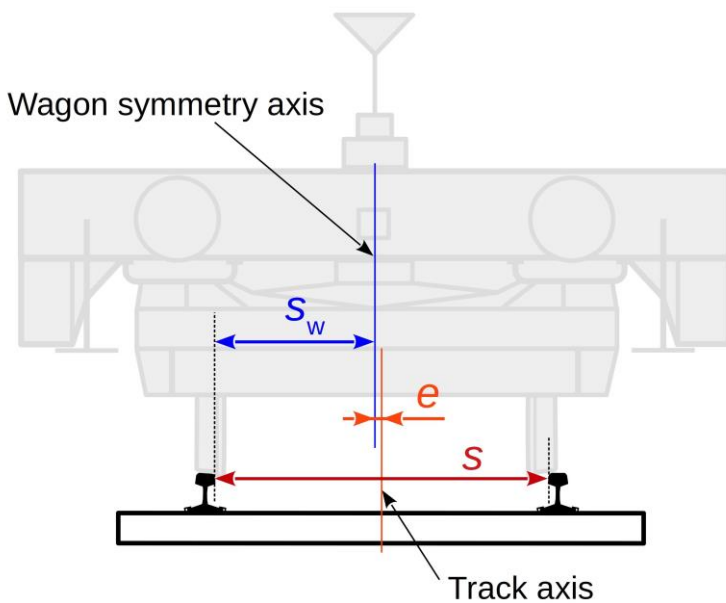

Fig. 5. Compensating lateral displacements of the measuring wagon.

The required value of the correction compensating lateral wagon displacements is calculated from the distance s between the two track rails, and the distance s_w between the symmetry axis of the wagon and one rail, according to the formula:

$$e = \frac{s}{2} - s_w \quad (8)$$

The relation (8) is valid for horizontal lateral orientation of the measuring wagon. When the wagon is tilted, e.g. when moving on arc, only the horizontal component e' of the compensating correction should be applied, according to the formula:

$$e' = e \cdot \cos \alpha = \left(\frac{s}{2} - s_w \right) \cdot \cos \alpha \quad (9)$$

In practice, the correction can always be calculated from formula (8), as for the maximum lateral wagon tilt and the displacement of 3 cm, the correction value calculated from formula (9) differs by about 0.1 mm from that obtained from formula (8). This difference is completely negligible, and ignoring it does not worsen the accuracy of the measurement in any way.

The other condition for the correction obtained from formula (8) to be sufficiently accurate is the parallelism of the track axis and the symmetry axis of the measuring wagon. This condition is not fulfilled on arcs. What is more, this parallelism of axes can also be lost on straight track sections, due to disturbances in wagon motion caused by its snaking, for instance. The loss of parallelism between the track axis and the wagon symmetry axis results in the appearance of measurement errors. To minimise them, measurements should be performed at pivot pin points, where GNSS receivers are installed in the way shown in Fig. 6.
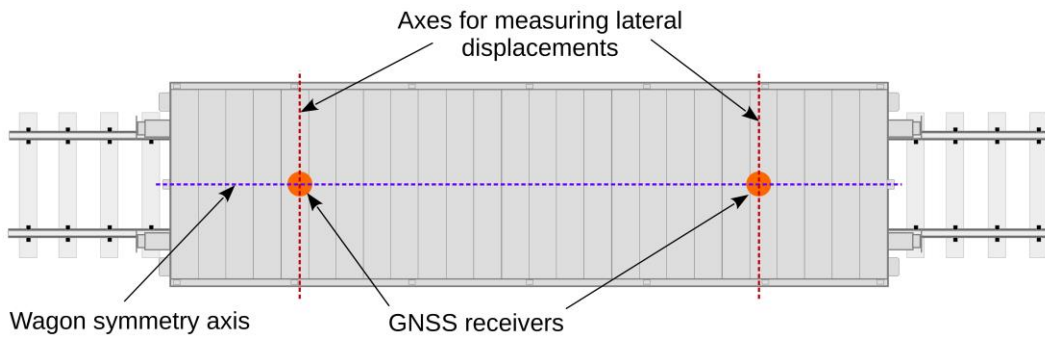
Fig. 6. Measuring points of lateral displacements of the measuring wagon

For measuring conditions in Fig. 6 on a straight track, the maximum errors resulting from non-parallelism of the wagon symmetry axis and the track axis are negligibly small, as they do not exceed 0.01 mm. On arch with a very small radius of $R = 150$ m they are slightly larger, but still do not exceed 0.5 mm. It is worth mentioning that, due to the dynamic operation of the wagon on the track, the lateral displacement correction coefficients should be calculated individually for each GNSS receiver.

2.3.3. Orientating the measuring wagon in the global coordinate system before calculating corrections for the determined coordinates

All corrections compensating dynamic movements of the measuring wagon are orientated in the local coordinate system, with one axis parallel to the track axis. Before using them for correcting coordinates recorded by GNSS receivers, they should be converted into the global system of satellite coordinates Y-East, X-North, consitituting reference for GNSS measurement results. To do that, we should know the current orientation of the measuring wagon in the global system. This orientation can be calculated based on the wagon's fixed base, as shown in Fig. 7.
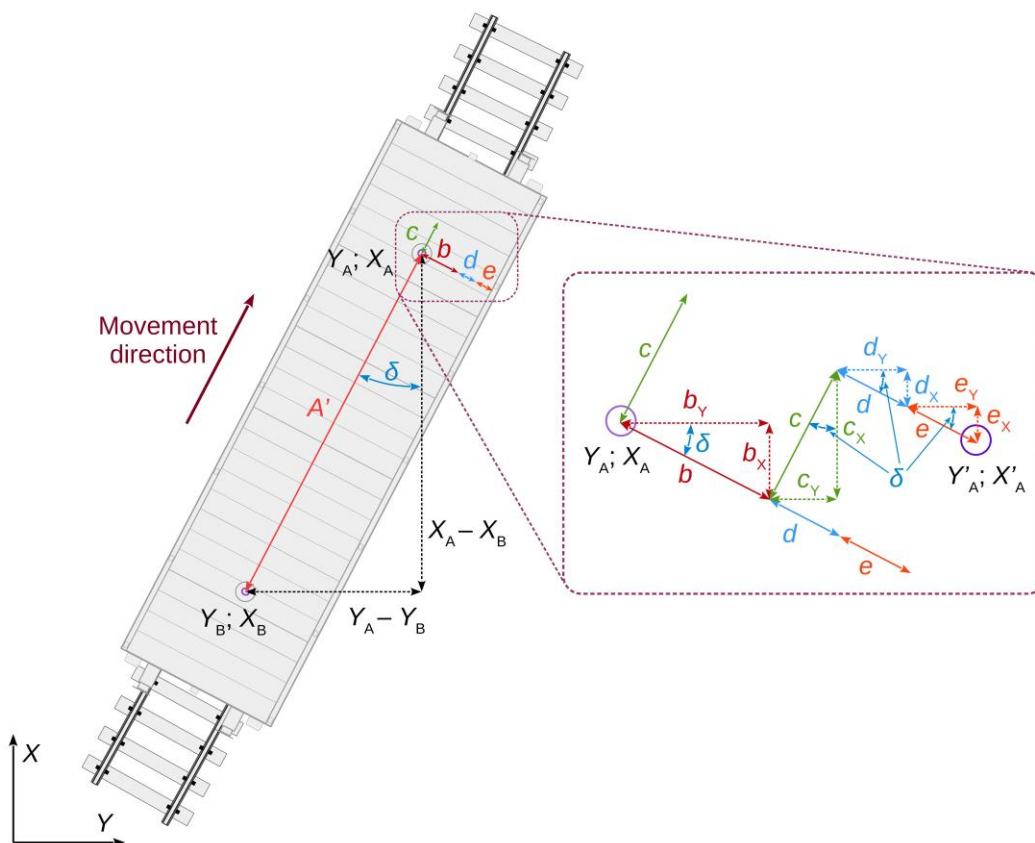
Fig. 7. Correction of satellite coordinates based on coefficients compensating dynamic motion of the measuring wagon (description in the text)

The orientation of the measuring wagon in the global coordinate system can be calculated using the positions of two satellite receivers installed at a given distance, i.e. the fixed base length A, from each other. The recorded coordinates Y_A, X_A of the first receiver and Y_A, X_A of the second receiver, along with the distance between them equal A', from the point of view of the constellation of satellites, provide exact global orientation of the fixed base, and, consequently, of the measuring wagon as a whole. The measure of this orientation is the angle δ. We can write that:

$$\sin \delta = \frac{Y_A - Y_B}{A'} = \frac{Y_A - Y_B}{A \cdot \cos \beta} \quad (10)$$

and:

$$\cos \delta = \frac{X_A - X_B}{A'} = \frac{X_A - X_B}{A \cdot \cos \beta} \quad (11)$$

After orientating the wagon in the global coordinate system, we can convert the compensating corrections into this system. For this purpose, the corrections b, c, d and e should be decomposed into components b_Y, c_Y, d_Y, e_Y and b_X, c_X, d_X, e_X respectively, taking into account the directions of Y- and X-axes in the global system (the values of corrections in Fig. 7 are not in scale with wagon dimensions). We can write:

$$b_Y = b \cdot \cos \delta = \frac{b}{A \cdot \cos \beta} \cdot (X_A - X_B) = \frac{h \cdot \sin \alpha}{A \cdot \cos \beta} \cdot (X_A - X_B) \quad (12)$$

$$c_Y = c \cdot \sin \delta = \frac{c}{A \cdot \cos \beta} \cdot (Y_A - Y_B) = \frac{h \cdot \sin \beta}{A \cdot \cos \beta} \cdot (Y_A - Y_B) = \frac{h}{A} \cdot \tan \beta \cdot (Y_A - Y_B) \quad (13)$$

$$d_Y = d \cdot \cos \delta = d \cdot \frac{X_A - X_B}{A \cdot \cos \beta} = \begin{cases} \left[\frac{l_p}{2} \cdot (1 - \cos \alpha) + w \cdot \sin \alpha \right] \cdot \frac{X_A - X_B}{A \cdot \cos \beta} & \text{for} \quad \alpha \geq 0 \\ -\left[\frac{l_p}{2} \cdot (1 - \cos \alpha) + w \cdot \sin |\alpha| \right] \cdot \frac{X_A - X_B}{A \cdot \cos \beta} & \text{for} \quad \alpha < 0 \end{cases} \quad (14)$$

$$e_Y = e \cdot \cos \delta = e \cdot \frac{X_A - X_B}{A \cdot \cos \beta} = \left(\frac{s}{2} - s_w \right) \cdot \frac{X_A - X_B}{A \cdot \cos \beta} \quad (15)$$

and:

$$b_X = b \cdot \sin \delta = \frac{b}{A \cdot \cos \beta} \cdot (Y_A - Y_B) = \frac{h \cdot \sin \alpha}{A \cdot \cos \beta} \cdot (Y_A - Y_B) \quad (16)$$

$$c_X = c \cdot \cos \delta = \frac{c}{A \cdot \cos \beta} \cdot (X_A - X_B) = \frac{h \cdot \sin \beta}{A \cdot \cos \beta} \cdot (X_A - X_B) = \frac{h}{A} \cdot \tan \beta \cdot (X_A - X_B) \quad (17)$$

$$d_X = d \cdot \sin \delta = d \cdot \frac{Y_A - Y_B}{A \cdot \cos \beta} = \begin{cases} \left[\frac{l_p}{2} \cdot (1 - \cos \alpha) + w \cdot \sin \alpha \right] \cdot \frac{Y_A - Y_B}{A \cdot \cos \beta} & \text{for} \quad \alpha \geq 0 \\ -\left[\frac{l_p}{2} \cdot (1 - \cos \alpha) + w \cdot \sin |\alpha| \right] \cdot \frac{Y_A - Y_B}{A \cdot \cos \beta} & \text{for} \quad \alpha < 0 \end{cases} \quad (18)$$

$$e_X = e \cdot \sin \delta = e \cdot \frac{Y_A - Y_B}{A \cdot \cos \beta} = \left(\frac{s}{2} - s_w \right) \cdot \frac{Y_A - Y_B}{A \cdot \cos \beta} \quad (19)$$

After calculating *X, Y* components of all corrections, the recorded coordinates of the receivers can be converted into the rail head plane. For receiver A, the following relations are valid:

$$Y_A' = Y_A + b_Y + c_Y + d_Y + e_Y \quad (20)$$

$$X_A' = X_A - b_X + c_X - d_X - e_X \quad (21)$$

After relevant substitutions and rearrangements, we obtain:

$$Y_A' = \begin{cases} Y_A + \dfrac{1}{A} \cdot \left\{ h \cdot \left[\dfrac{\sin \alpha}{\cos \beta} \cdot (X_A - X_B) + \tan \beta \cdot (Y_A - Y_B) \right] + \dfrac{X_A - X_B}{\cos \beta} \cdot \left[\dfrac{l_p}{2} \cdot (1 - \cos \alpha) + w \cdot \sin \alpha + \dfrac{s}{2} - s_w \right] \right\} & \text{for} \quad \alpha \geq 0 \\[3mm] Y_A + \dfrac{1}{A} \cdot \left\{ h \cdot \left[\dfrac{\sin \alpha}{\cos \beta} \cdot (X_A - X_B) + \tan \beta \cdot (Y_A - Y_B) \right] + \dfrac{X_A - X_B}{\cos \beta} \cdot \left[-\dfrac{l_p}{2} \cdot (1 - \cos \alpha) - w \cdot \sin |\alpha| + \dfrac{s}{2} - s_w \right] \right\} & \text{for} \quad \alpha < 0 \end{cases}$$

(22)

$$X_A' = \begin{cases} X_A + \dfrac{1}{A} \cdot \left\{ h \cdot \left[-\dfrac{\sin \alpha}{\cos \beta} \cdot (Y_A - Y_B) + \tan \beta \cdot (X_A - X_B) \right] - \dfrac{Y_A - Y_B}{\cos \beta} \cdot \left[\dfrac{l_p}{2} \cdot (1 - \cos \alpha) + w \cdot \sin \alpha + \dfrac{s}{2} - s_w \right] \right\} & \text{for} \quad \alpha \geq 0 \\[3mm] X_A + \dfrac{1}{A} \cdot \left\{ h \cdot \left[-\dfrac{\sin \alpha}{\cos \beta} \cdot (Y_A - Y_B) + \tan \beta \cdot (X_A - X_B) \right] - \dfrac{Y_A - Y_B}{\cos \beta} \cdot \left[-\dfrac{l_p}{2} \cdot (1 - \cos \alpha) - w \cdot \sin |\alpha| + \dfrac{s}{2} - s_w \right] \right\} & \text{for} \quad \alpha < 0 \end{cases}$$

(23)

The relations (22) and (23) convert the calculated coordinates into the design axis position. When determining the real axis position, the correction *d* is omitted, which simplifies these relations to the form:

$$Y_A' = Y_A + \dfrac{1}{A} \cdot \left\{ h \cdot \left[\dfrac{\sin \alpha}{\cos \beta} \cdot (X_A - X_B) + \tan \beta \cdot (Y_A - Y_B) \right] + \dfrac{X_A - X_B}{\cos \beta} \cdot \left(\dfrac{s}{2} - s_w \right) \right\} \quad (24)$$

$$X_A' = X_A + \dfrac{1}{A} \cdot \left\{ h \cdot \left[-\dfrac{\sin \alpha}{\cos \beta} \cdot (Y_A - Y_B) + \tan \beta \cdot (X_A - X_B) \right] - \dfrac{Y_A - Y_B}{\cos \beta} \cdot \left(\dfrac{s}{2} - s_w \right) \right\} \quad (25)$$

For receiver B, these relations are identical. Only the value of correction *e* related to lateral displacement can be different.

3. Experimental verification

To verify the theoretical assumptions presented above, measurements were performed on selected railway lines no. 211 and no. 203, courtesy of Zakład Linii Kolejowych PKP PLK in Gdynia, and using the rolling stock owned by PKP PLK and Pomorskie Przedsiębiorstwo Mechaniczno-Torowe (PPMT) in Gdansk. The measuring train consisted of a 4-axial wagon-platform 401Z, on which the measuring and recording equipment was installed, a separating 2-axial wagon-platform, and a DH-350 motor car used as the traction vehicle. The additional separating wagon was used to provide the same measuring conditions for the two main GNSS receivers. Without the separating wagon, the receiver situated closer to the motor car would have worse conditions for measurements due to the presence of the motor car cab, which could obscure the satellites. The view of the measuring train is shown in Fig. 8.

Fig. 8. View of the measuring train.

The applied GNSS receivers, model R10, made by Trimble, were placed above bogie pivot axes (main receivers) and above the rails, at points on the lines perpendicular to wagon axis and passing through bogie pivot points (supplementary receivers). The height of the receivers mounted above the rail head was $h = 1.64$ m. In turn, the height of the track surface at the place of measurement was $w = 0.369$ m. The distance between the bogie pivot axes for the wagon which was used is 7 m and it is equal to the length of the fixed base A. This length was determined by using the first class precision tape measure with standard uncertainty equal $u(A) \approx 0.5$ mm. Lateral and longitudinal tilts of the wagon were measured with a dynamic inclinometer SICK TM88D, installed close to one of the GNSS receivers. The signals from the inclinometer and other measuring devices were recorded by a computer, using in-house software developed in LabVIEW environment. The arrangement of basic measuring instruments is shown in Fig. 9.
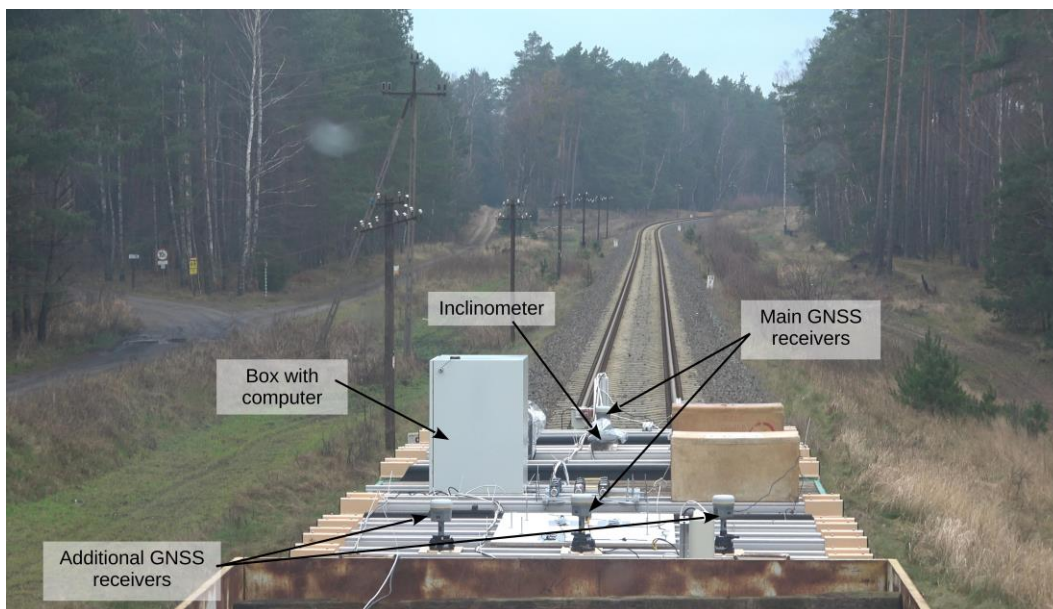
Fig. 9. Arrangement of basic measuring instruments on the wagon

The main measurements covered a railway line section consisting of two straight sections and a circular arc, linked together by transition curves. The measurements were performed at constant speed $v = 10$ km/h of the measuring wagon. Low riding speed allowed for minimising the influence of centrifugal force occurring in the arches on the angle measurement results obtained from the

inclinometer made in micro-electro-mechanical systems (MEMS) technology. The tests performed for higher speeds have shown the need to use a different technology for measuring longitudinal and lateral angles, which will be the subject of further research.

3.1. Measuring longitudinal track inclination and compensating its effect on measurement results

The examined railway line section had moderate longitudinal inclinations, with values not exceeding $i_{max} = 11\text{‰}$. Having been recalculated into angular measures, the inclination did not exceed $\beta = 0.63°$. Despite such a small value of the inclination angle, it could be measured using the inclinometer. The results of this measurement are shown in Fig. 10, which also presents the comparison of the measured angle with theoretical values obtained from technical documentation of this railway line.
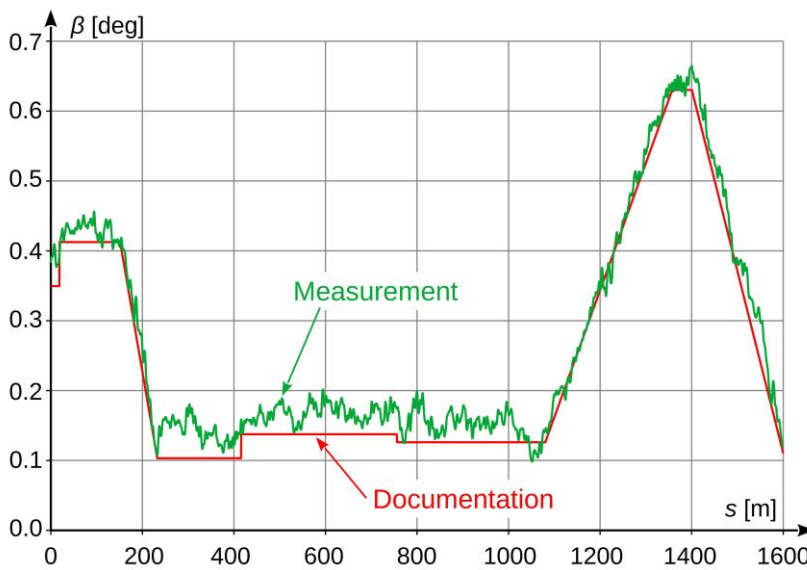
Fig. 10. Results of measurement of longitudinal inclination angle β

As shown in Fig. 10, the measured longitudinal inclination angles show very good compatibility with theoretical values. This confirms the possibility of recording these inclinations with an inclinometer, and demonstrates the compliance of real geometric parameters of the examined line with its technical documentation.

With the measured value of the longitudinal inclination angle, we can calculate the correction c from formula (5), and decompose it into axial components c_Y and c_X, according to relations (13) and (17), respectively. The values of correction c and its components are shown in Fig. 11.
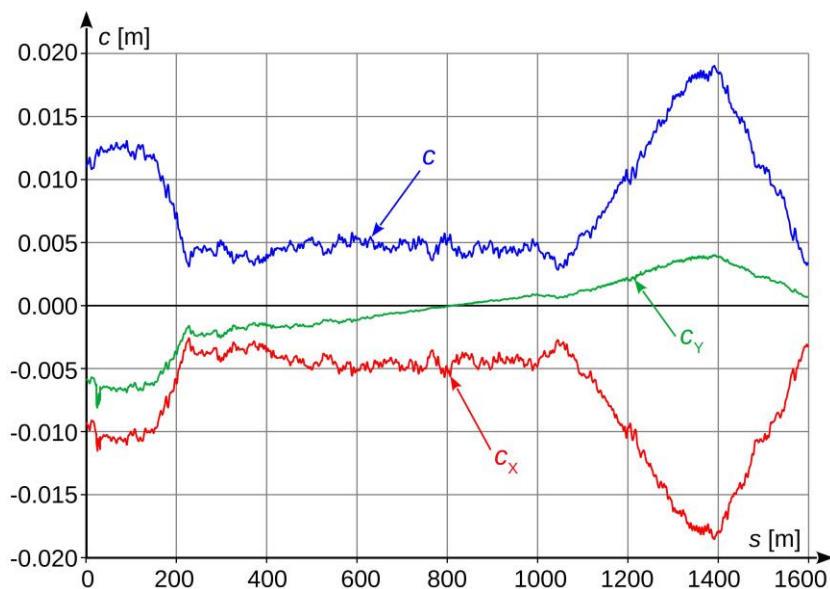
Fig. 11. Values of correction c and its components c_Y and c_X

For the longitudinal inclinations recorded on the examined railway line section, the maximum value of correction c slightly exceeds 15 mm. Its effect on the railway track axis measurement result is very small, but it should be taken into account when high precision of measurements is expected.

3.2. Measuring lateral track inclination and compensating its effect on measurement results

Unlike longitudinal inclinations, the measuring wagon tilts resulting from lateral track inclinations on arcs reach much higher values and, consequently, their effect on measurement results is greater. The lateral track inclination recorded on the arc of the examined railway line section was 50 mm, which gives $\alpha = 1.91°$ in angular measures. These values are higher by one order of magnitude on the corresponding values for longitudinal inclination. The measured lateral inclination angles are shown and compared with values from technical documentation in Fig. 12.
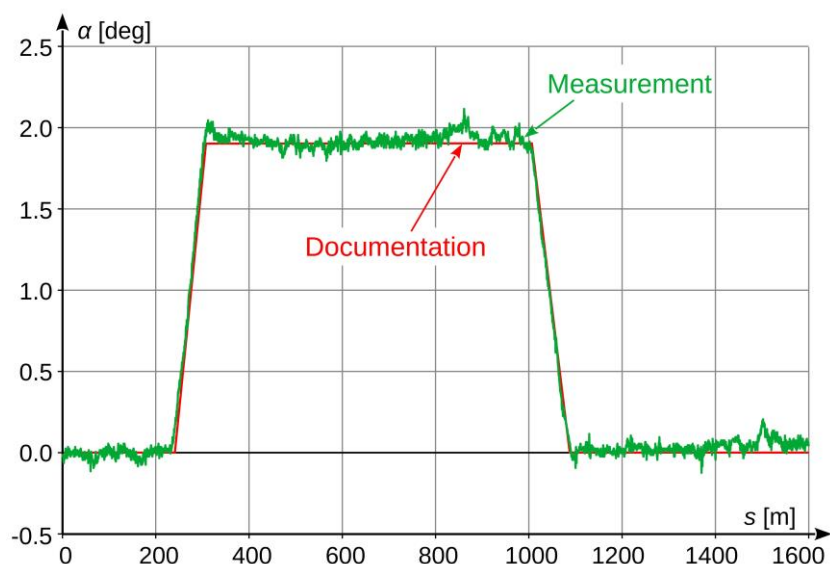
Fig. 12. Results of measurement of lateral inclination angle α and their comparison with the data from technical documentation

Like in case of longitudinal inclinations, good compatibility is observed between the measured results and the technical documentation of the examined railway line.

The measured values of the lateral inclination angle form the basis for calculating corrections b and d. Since these two corrections are proportional to the inclination angle value, they will only differ from each other only by absolute value (the same applies to their components b_Y, b_X and d_Y, d_X). The values of these corrections are shown in Figs. 13 and 14.
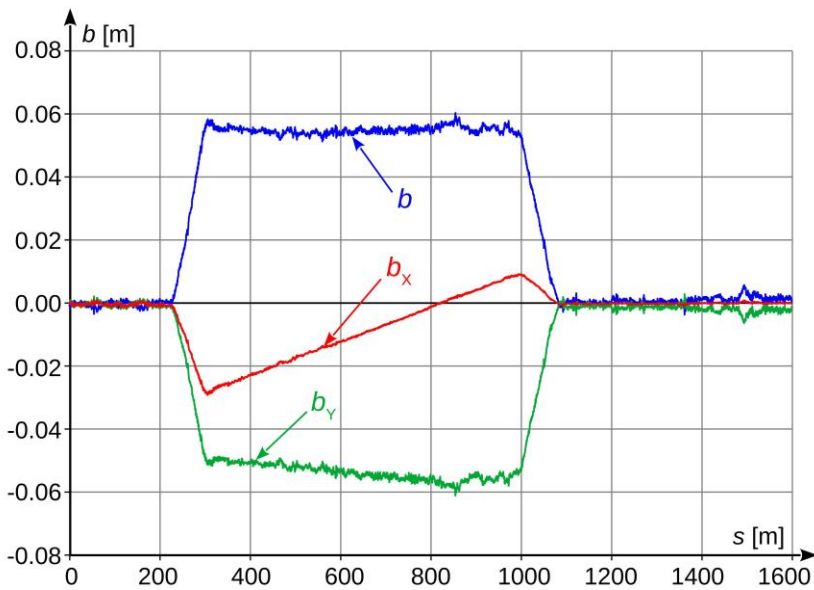

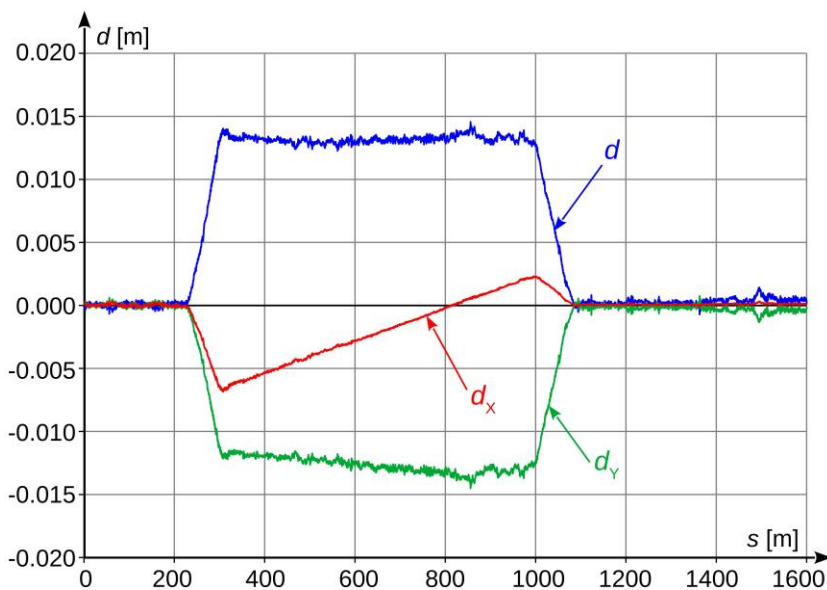Fig. 13. Values of correction b and its components b_Y and b_X

Fig. 14. Values of correction d and its components d_Y and d_X

Figures 13 and 14 show that the total value of corrections b and d lies within the range of a few centimetres. Therefore, it definitely must be taken into consideration when measuring the railway track axis position.

3.3. Measuring lateral wagon displacements and compensating their effect on measurement results

Lateral displacements of the measuring wagon were measured using the visual system consisting of two cameras, situated at opposite ends of the wagon, as shown in Fig. 15.
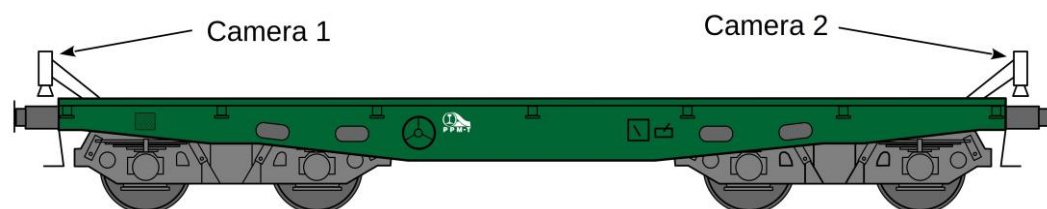
Fig. 15. Distribution of cameras used to create the visual system for measuring lateral displacements of the measuring wagon

Since the lateral displacements were measured at the wagon's ends, and not at bogie pivot axis points, their values required corrections to compensate the displacements of the wagon's ends with respect to the track axis on arcs, as shown in Fig. 16.
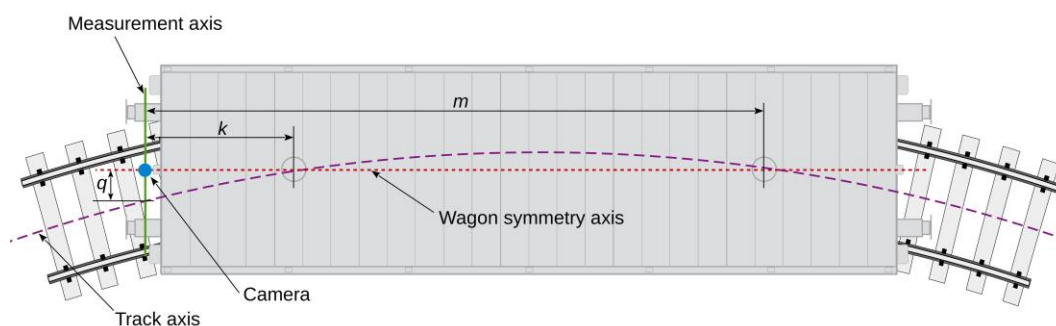

Fig. 16. Correction of the lateral displacement signal obtained from measuring cameras situated at opposite ends of the wagon

The value of correction q shown in Fig. 16 depends on the current track arc radius and is given by the following formula:

$$q = \sqrt{\frac{-\left(k^2 + m^2 - 4 \cdot R^2\right) - \sqrt{\left(k^2 + m^2 - 4 \cdot R^2\right)^2 - 4 \cdot k^2 \cdot m^2}}{2}} \quad (26)$$

where: k – distance from the measuring point (camera axis position) to the closer pivot axis; m – distance from the measuring point to the more distant pivot axis; R – arc radius.

In order to obtain the value of the correction e while driving on arch, the value of the correction q should be subtracted from the obtained measurement result.

The measured correction e, taking into account the correction resulting from the formula (26), is shown in Fig. 17, along with its components e_Y and e_X.
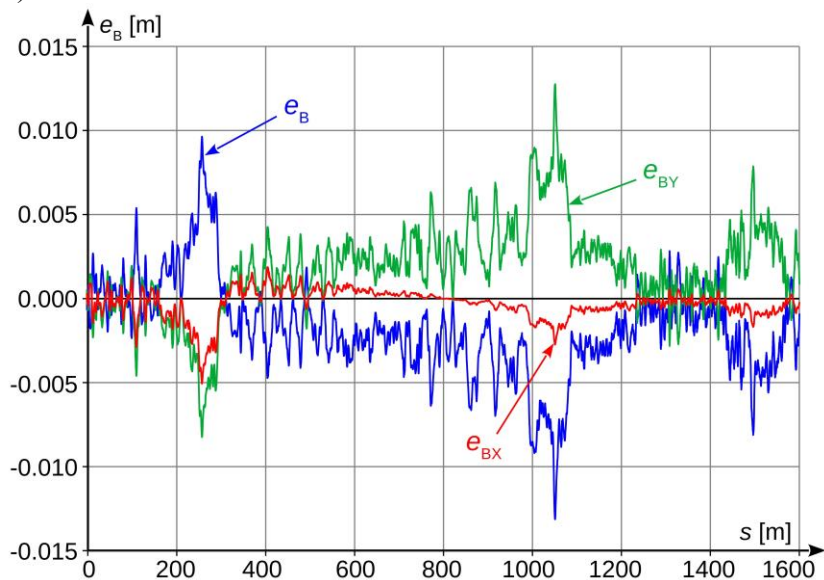
a)
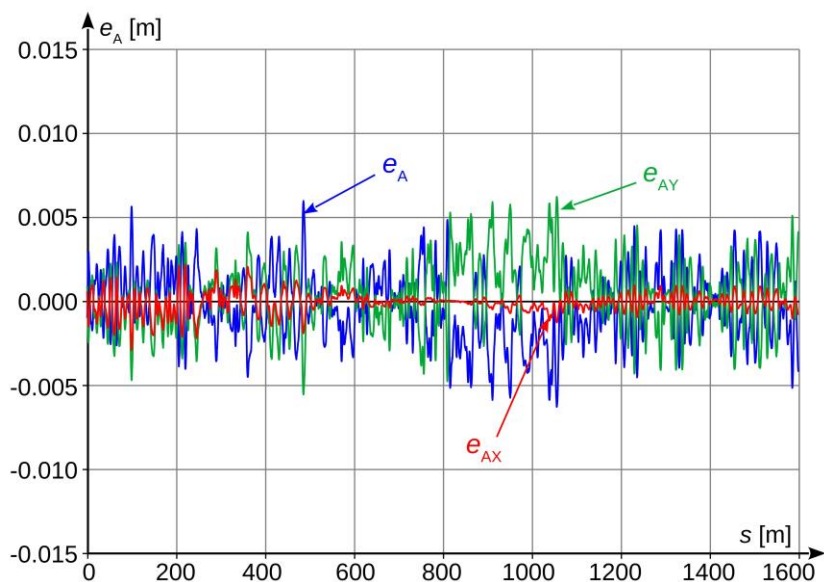
Fig. 17. Values of correction e and its components e_Y and e_X: a) for receiver A; b) for receiver B

Figure 17 shows that the value of correction e does not exceed 5 mm in most cases, and only temporarily reaches the level of 10–13 mm. In the absolute scale, it is the smallest of all corrections used for compensating the results of railway track axis measurements. In practice, the validity of taking into consideration such small corrections is questionable. It can be justified only in situations when the quality of the position signal coming from GNSS receivers is at a very high level. For a worse-quality signal, statistical dispersion of the results coming from satellite receivers will be greater than the above correction, hence taking it into consideration in such a situation is purposeless.

3.4. Summary compensation of the effect of wagon body displacement on measurement results

Figure 18 compares the railway track axis measurement results recorded directly by the GNSS receivers with those obtained after introducing compensating corrections. The introduced corrections are shown for the arc and for the straight track section. In the latter case, the track section with the greatest longitudinal inclination was selected.
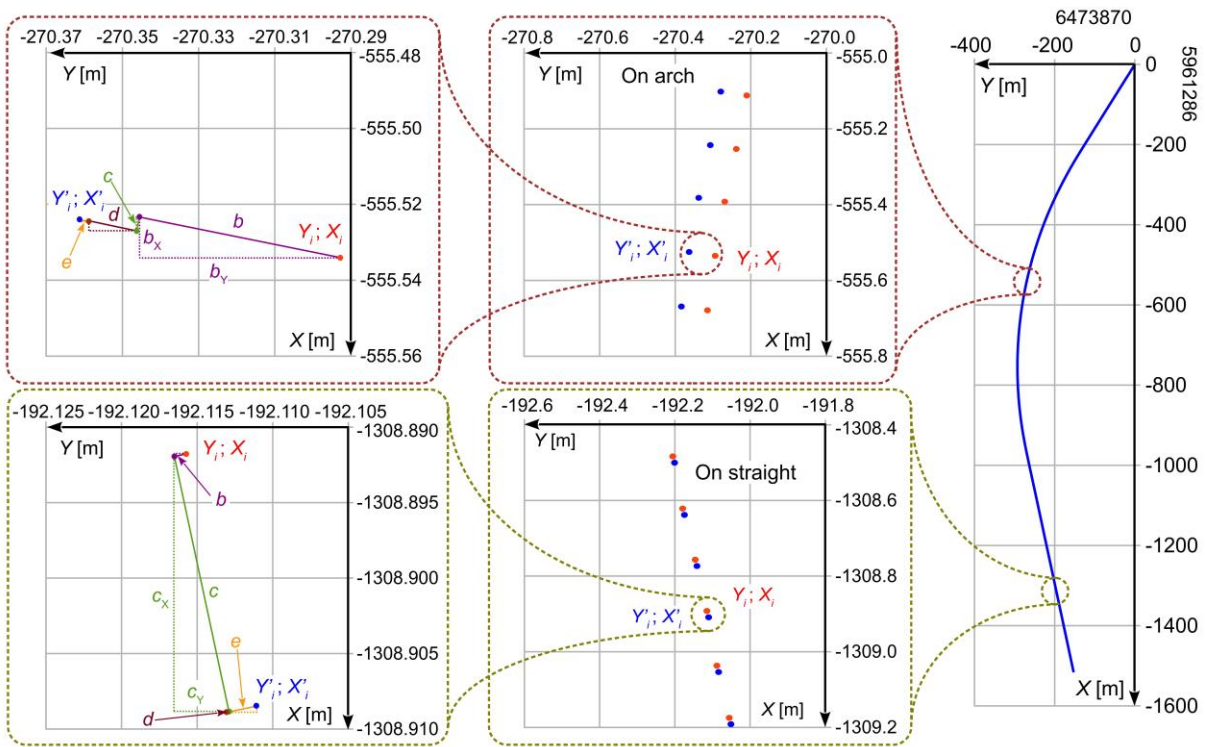
Fig. 18. Compensating the results of railway track axis measurement

Figure 18 shows that when the measuring wagon moves on the arc, the corrections *b* and *d* dominate. This is because they are directly related to the presence of lateral track inclination. On the other hand, when the measuring wagon moves on the straight track section, the values of these corrections are the smallest, as they reflect only minor imperfections in track geometry. The presence and values of correction *c* are directly related to longitudinal track inclinations.

3.5. Uncertainty assessment of coordinate determination

To assess the uncertainty of coordinate determination, the experimental standard deviation was calculated as the moving function from the formula (3). This means that, for each measuring point, the deviation was calculated within the interval of ± 15 samples in the vicinity of this point. The results of the performed calculations are shown in Fig. 19.
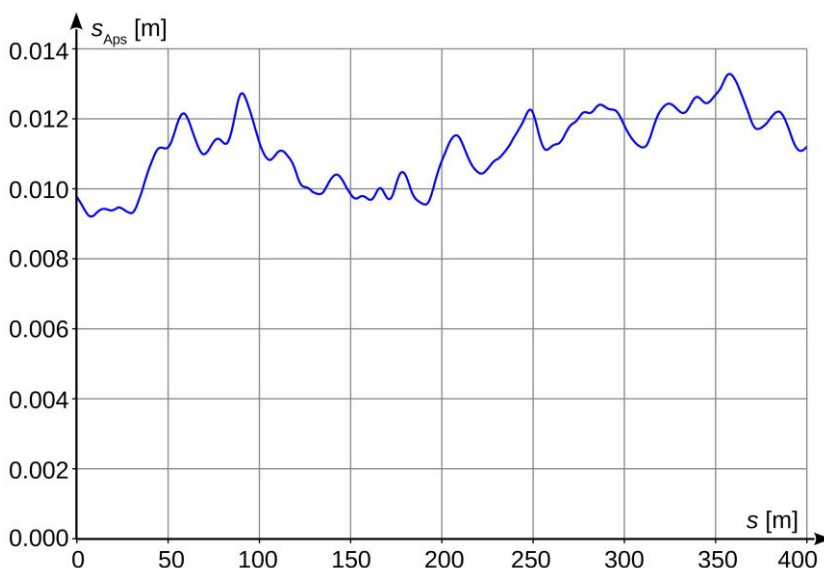
Fig. 19. Experimental standard deviation for fixed base length measurement based on coordinates recorded by main GNSS receivers

The constant and small value of the experimental standard deviation along the entire examined track section correlates to a relatively constant and large number of observed satellites (Fig. 20). That means, when the measuring wagon moved along the track section, that there were no field screens, which would dramatically change the observed horizon area. The value of the Horizontal Dilution of Precision (HDOP) coefficient was also relatively constant and very low, below 1, which indicates excellent geometry of the GNSS space segment – Fig. 21. This means that either there were no moving field screens, or they were small and favourably situated. The analysis of HDOP coefficients allows us to conclude that high reliability of the obtained measurement results can be ensured by favourable conditions, hence the measuring campaigns should be planned in such a way as to obtain the best possible geometric coefficients.
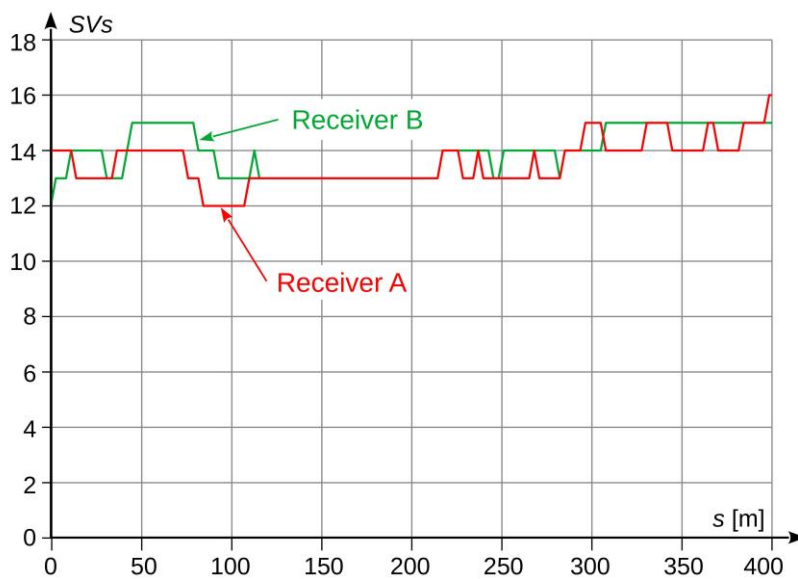

Fig. 20. Number of satellites used by GNSS receivers along the test section
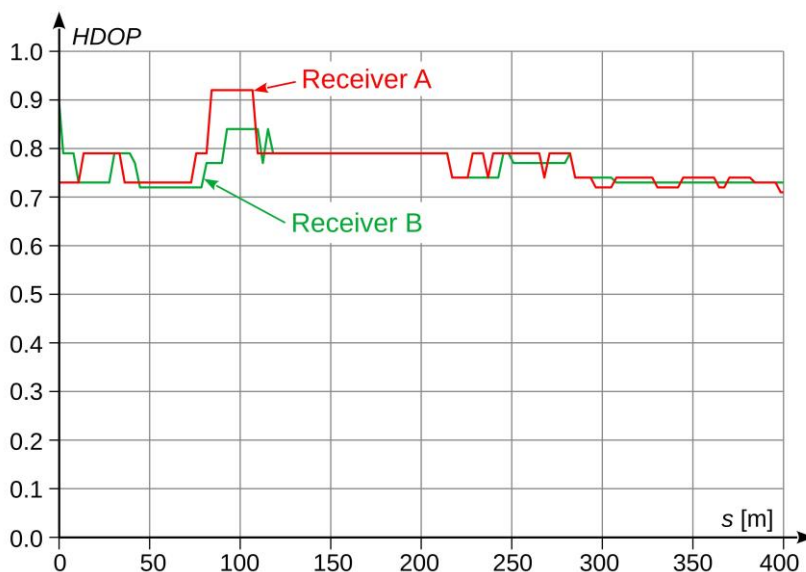

Fig. 21. Distribution of HDOP values along the test section

4. Summary and conclusions

The results of experimental measurements presented in the article testify to the fact that the proposed innovative method to determine the railway track axis based on the fixed base of the measuring vehicle offers a number of advantages, compared to earlier methods. The use of two GNSS receivers situated above the pivot axes of the vehicle, at the known and relatively large distance, counted in meters, significantly improve the precision and simplify the calculations of positioning corrections related to longitudinal and lateral wagon tilts resulting from a given track profile and the presence of lateral track inclinations on arcs. These advantages are particularly noticeable in comparison to all the methods using manually driven measuring trolleys. Small dimensions of these trolleys, especially the length, necessarily have a negative effect on the accuracy of determining spatial orientation of GNSS receivers [6–9]. Another important factor is the possibility of the operator's presence, which has negative impact on the quality of the signal received by GNSS receivers (they are obscured). This does not occur when a wagon is used. Whether to consider, lateral displacements of the measuring vehicle body, which are determined with the use of visual techniques, remains an open question, as the calculated values of these displacements are very small. It is also worth mentioning that the fixed base allows for to conducting permanent control of the metrological quality of the performed measurement. Based on the standard deviation of the fixed base length, standard uncertainty of determining the position of the track axis can be estimated at $u(X) \approx u(Y) \approx 12$ mm. The accuracy of the measurement is therefore about an order of magnitude worse than that obtained when measuring trolleys are used [7], but the measuring efficiency (speed) is ten times higher than in the method mentioned above (10 km/h versus 1 km/h). Ultimately, it is planned to increase it several times up, to the level of 30–50 km/h.

Further research work in this area will focus on improving the accuracy of measuring wagon position determination, and on developing software intended to facilitate the measurement data analysis process. Practical implementation of the developed method of railway track axis measurement will accelerate significantly the processes of diagnosing and monitoring technical condition of railway track surfaces, and will make them more reliable.

Credit author statement: **Andrzej Wilk:** Conceptualisation, Methodology, Project administration; Supervision **Władysław Koc:** Conceptualisation, Methodology, Writing – Review & Editing; Supervision **Cezary Specht:** Methodology, Resources, Supervision, **Jacek Skibicki:** Methodology, Formal analysis, Software, Investigation, Writing – Original Draft, Visualisation, **Slawomir Judek:** Software, Investigation, Writing – Review & Editing, Visualisation; **Krzysztof Karwowski:** Investigation, Resources, **Piotr Chrostowski:** Investigation, Writing – Original Draft, **Jacek Szmagliński:** Investigation, **Paweł Dąbrowski:** Software, Investigation, **Krzysztof Czaplewski:** Software, Investigation, **Mariusz Specht:** Software, Investigation, **Roksana Licow:** Investigation, **Sławomir Grulkowski:** Resources.

5. References

[1]   E. Bongini, E. Bonnet, Railway noise sources definition within the scope of pass-by sound synthesis, in: Euronoise 2009, 8th European conference on noise control, Edinburgh, Scotland; 2009.

[2]   S. Kaeeni, M. Khalilian, J. Mohammadzadeh, Derailment accident risk assessment based on ensemble classification method, Safety Science, Volume 110, Part B, 2018, pp. 3–10. ISSN 0925-7535.

[3]   X. Qing-yuan, O. Xi, F.T.K. Au, L. Ping, X. Zu-cai, Effects of track irregularities on environmental vibration caused by underground railway, European Journal of Mechanics - A/Solids, Volume 59, 2016, pp. 280–293. ISSN 0997-7538.

[4]   Y.B. Yang, H.H. Hung, Wave propagation for train-induced vibrations. A Finite/Infinite Element Approach, World Scientific Publishing Co. Pte. Ltd. Singapore 2009. ISBN-13 978-981-283-582-6. https://doi.org/10.1142/7062.

[5]   O. Javaid, D.H. Choi, Effect of track irregularities on the response of two-way railway tracks, Applied Science. 2020, 10(1), 11. https://doi.org/10.3390/app10010011.

[6]   S.B. Chiou, J.Y Yen, Precise railway alignment measurements of the horizontal circular curves and the vertical parabolic curves using the chord method, Proceedings of the Institution of Mechanical Engineers, Part F: Journal of Rail and Rapid Transit 2019, 233 (5), pp. 537–549. doi:10.1177/0954409718800527.

[7]   H. Tsunashima, Y. Naganuma, T. Kobayashi, Track geometry estimation from car-body vibration, Journal Vehicle System Dynamics, International Journal of Vehicle Mechanics and Mobility, 2014, 52:sup1, pp.207–219. doi: 10.1080/00423114.2014.889836.

[8]   H. Tsunashima, Condition monitoring of railway tracks from car-body vibration using a machine learning technique, Applied Sciences, 2019, 9, 2734. doi: 10.3390/app9132734.

[9]   X. Xiao, Z. Sun, W. Shen, A Kalman filter algorithm for identifying track irregularities of railway bridges using vehicle dynamic responses. Mechanical Systems and Signal Processing, vol. 138, 2020. doi: 10.1016/j.ymssp.2019.106582.

[10] B. Akpinar, E. Gülal, Multisensor railway track geometry surveying system, IEEE Transactions on Instrumentation and Measurement, vol. 61, no. 1/2012, pp. 190–197. doi: 10.1109/TIM.2011.2159417.

[11] R. Li, Z. Bai, B. Chen, H. Xin, Y. Cheng, Q. Li, F. Wu, High-speed railway track integrated inspecting by GNSS-INS multisensor, in 2020 IEEE/ION Position, Location and Navigation Symposium (PLANS), Portland USA, 2020. doi: 10.1109/PLANS46316.2020.9109908.

[12] Y. Zhou, Q. Chen, X. Niu, Kinematic measurement of the railway track centerline position by GNSS/INS/odometer integration, IEEE Access 2019, 7, pp. 157241–157253. doi:10.1109/ACCESS.2019.2946981.

[13] Q. Chen, X. Niu, L. Zuo, T. Zhang, F. Xiao, Y. Liu, J. Liu, A railway track geometry measuring trolley system based on aided INS, Sensors 2018, 18 (2), 538. https://doi.org/10.3390/s18020538.

[14] A. Moskal, E. Pastucha, Track and gauge geometry measurements – the present and future, Measurement Automation Monitoring, Feb. 2016, vol. 62, ISSN 2450-2855, no. 02, pp. 66–71.

[15] E. Sackl, The EM-SAT 120 track survey car, an integrated part of the track geometry data base of the Austrian Federal Railways ÖBB, Rail Technology Review, 2/2004, pp. 39–43.

[16] H. Wirth, Der neue Lichtraummesszug LIMEZ III der Deutschen Bahn AG, ZFV 3/2008 133. Jg, pp.180–186.

[17] H. Tanaka, T. Otake, Y. Naganuma, M. Goto, Development of a new track inspection car for the Tokaido and Sanyo Shinkansen, Proc. of The Railway Technology Conference, 2000.

[18] D. Sakuta, K. Hamaoka, Y. Akashi, K. Tanaka, Development and deployment of track inspection technique on in-service rolling stock. Hitachi Review 2018, vol. 67, no. 7, pp. 83–88.

[19] T Hisa, M Kanaya, M Sakai, K Hamaoka, Rail and contact line inspection technology for safe and reliable railway traffic, Hitachi Review 2012, vol. 61, no. 7, pp. 325–330.

[20] R.S. Barbosa, New method for railway track quality identification through the safety dynamic performance of instrumented railway vehicle, Journal of the Brazilian Society of Mechanical Sciences and Engineering 2016, 38 (8), pp. 2265–2275. doi:10.1007/s40430-015-0471-9.

[21] M. Moretti, M. Triglia, G. Maffei, ARCHIMEDE – the first European diagnostic train for global monitoring of railway infrastructure, IEEE Intelligent Vehicles Symposium, Parma, 2004, pp. 522-526. doi: 10.1109/IVS.2004.1336438.

[22] A.A. Minina, E.N. Zhdanova, R.V. Shalymov, Subsystem on-board information-measuring system, 2018 IEEE International Conference "Quality Management, Transport and Information Security, Information Technologies" (IT&QM&IS), St. Petersburg, 2018, pp. 248–252. doi: 10.1109/ITMQIS.2018.8525090.

[23] D. Giorgio, F. Cheli, A. Collina, F. Resta, P. Belforte, F. Favo, A. Fumi, Railway line and overhead equipment diagnostics through onboard high speed laboratory train, 8th World Congress on Railway Research (WCRR), Seoul 2008.

[24] D. Giorgio, F. Cheli, P. Belforte, F. Resta, M. Elia, F. Favo, Diagnostic train for high speed line: a tool for improving vehicle and track maintenance, ASME 2007 International Mechanical Engineering Congress and Exposition, Seattle, 2007. doi: 10.1115/IMECE2007-42694.

[25] Q. Chen, X Niu, Q. Zhang, Y. Cheng, Railway track irregularity measuring by GNSS/INS integration, Navigation 2015, 62 (1), pp. 83–93. doi:10.1002/navi.78.

[26] Q. Zhang, Q. Chen, X. Niu, C. Shi, Requirement assessment of the relative spatial accuracy of a motion-constrained GNSS/INS in shortwave track irregularity measurement, Sensors 2019, 19 (23), 5296. doi:10.3390/s19235296.

[27] A. Wilk, C. Specht, W. Koc, K. Karwowski, P. Chrostowski, J. Szmagliński, P. Dąbrowski, M. Specht, S. Judek, J. Skibicki, M. Skóra, S. Grulkowski, Research project BRIK: development of an innovative method for determining the precise trajectory of a railway vehicle, Transportation Overview - Przegląd Komunikacyjny 2019, (7), pp. 32–47. doi:10.35117/A_ENG_19_07_04.

[28] J. Otegui, A. Bahillo, I. Lopetegi, L.E. Diez, Evaluation of experimental GNSS and 10-DOF MEMS IMU measurements for train positioning, IEEE Transactions on Instrumentation and Measurement 2019, 68 (1), pp. 269–279. doi:10.1109/TIM.2018.2838799.

[29] E. González, C. Prados, V. Antón, B. Kennes, GRAIL-2: enhanced odometry based on GNSS, Procedia - Social and Behavioral Sciences 2012, 48, pp. 880–887. doi: 10.1016/j.sbspro.2012.06.1065.